



This is the accepted manuscript made available via CHORUS. The article has been published as:

Optimal entangling operations between deterministic blocks of qubits encoded into single photons

Jake A. Smith and Lev Kaplan

Phys. Rev. A **97**, 012320 — Published 16 January 2018

DOI: [10.1103/PhysRevA.97.012320](https://doi.org/10.1103/PhysRevA.97.012320)

Optimal Entangling Operations between Deterministic Blocks of Qubits Encoded into Single Photons

Jake A. Smith^{1,*} and Lev Kaplan¹

¹*Tulane University, Department of Physics, New Orleans, Louisiana 70118, USA*

(Dated: January 2, 2018)

Here, we numerically simulate probabilistic elementary entangling operations between rail-encoded photons for the purpose of scalable universal quantum computation or communication. We propose grouping logical qubits into single-photon blocks wherein single-qubit rotations and the CNOT gate are fully deterministic and simple to implement. Inter-block communication is then allowed through said probabilistic entangling operations. We find a promising trend in the increasing probability of successful inter-block communication as we increase the number of optical modes operated on by our elementary entangling operations.

I. INTRODUCTION

Since the discovery of several high-profile quantum algorithms in the 1990s, there has been significant interest in developing programmable quantum hardware that is both reliable and scalable. One particular approach has been the linear optical quantum computing paradigm, where qubits are encoded into the spatial and polarization states of a small number of photons. The advantage to using photons is that they tend to not interact with their environment and optical quantum states are thus naturally resistant to decoherence [1]. On the other hand, photon-photon interaction is weak and linear entangling operations are limited to bosonic interference effects [1, 2]. Early proposals for an optical quantum computer circumvented this problem by encoding information into the degrees of freedom of a single photon, but this approach limited scalability [3–5]. In 2001, Knill, Laflamme, and Milburn discovered that universal entangling operations between a pair of qubits encoded into separate photons could be achieved probabilistically using ancilla photons and partial measurements [6, 7]. Still, experimental efforts continue to develop and use single-photon devices, often for specialized applications [8–15].

In our work here, we explore a balance between the reliability of single photon computing and the scalability of multi-photon computing. We propose encoding a few qubits into single-photon blocks so that within each block “entangling” operations between qubits are carried out through simple deterministic linear elements. Success of this model depends completely on reliable communication between blocks, which is accomplished through photon-pair entangling operations. Here, we numerically test our ability to carry out these inter-block operations using only linear optical circuit elements (i.e., beam splitters and phase shifters), ancilla states, and probabilistic partial measurements.

This paper is organized as follows: in Sections II

and III we review mathematical definitions and introduce methods for simulating linear optical quantum circuits. Then, in Section IV, we discuss the single-photon block encoding model in detail. In Sections V–VI we present a formalism for describing the most fundamental entangling operations between pairs of photons. Finally, in Sections VII–VIII we present our results.

II. MATHEMATICAL BACKGROUND

An optical quantum state of N photons contained in M optical modes can be written in the Fock basis,

$$|\psi\rangle = c_1 |N_1, 0_2, \dots, 0_M\rangle + c_2 |N-1_1, 1_2, 0_3, \dots, 0_M\rangle \dots + c_{d_H} |0_1, 0_2, \dots, N_M\rangle, \quad (1)$$

where the Hilbert space dimension of the system is given by

$$d_H = \frac{(N+M-1)!}{N!(M-1)!} \quad (2)$$

or the number of ways to order N indistinguishable photons and $M-1$ partitions.

A linear optical operation acting on a quantum state is generally described by the transformation of creation operators [1, 16]:

$$\hat{a}_\alpha^\dagger \rightarrow \sum_{\beta=1}^M U_{\alpha\beta} \hat{a}_\beta^\dagger, \quad (3)$$

where $U_{\alpha\beta}$ are the elements of a unitary complex matrix, U . One typically writes a state given by Eq. (1) as

$$|\psi\rangle = \left[c_1 \frac{(\hat{a}_1^\dagger)^N}{\sqrt{N!}} + c_2 \frac{(\hat{a}_1^\dagger)^{N-1} \hat{a}_2^\dagger}{\sqrt{(N-1)!}} + \dots \right. \\ \left. + c_{d_H} \frac{(\hat{a}_M^\dagger)^N}{\sqrt{N!}} \right] |0, 0, \dots, 0_M\rangle \quad (4)$$

and applies the symbolic transformation, Eq. (3). For large N and M , however, this process can quickly become

*Electronic address: jsmith74@tulane.edu

intractable. Here, we use an efficient and highly parallelizable numerical protocol for simulating linear optical quantum gates or state evolution that is equivalent to the action of Eq. (3), but can effectively handle large values of N and M . We will present this protocol in its entirety in Section III.

Before we begin, we define $A(U)$ as the unitary matrix which represents the action of Eq. (3) on a quantum state in the Fock basis (1). The output state $|\psi'\rangle$ of a linear optical circuit will be determined by standard matrix-vector multiplication,

$$|\psi'\rangle = A(U) |\psi\rangle. \quad (5)$$

If $N \geq 2$, the group $\mathbf{A} = \{A(U)\}$ of all possible linear optical operators is a proper (strict) subgroup of the unitary group,

$$\mathbf{A} \subset \mathbf{U}(d_H). \quad (6)$$

In other words, not all quantum transformations on multi-photon Fock states can be implemented via linear optical circuits. Indeed, the condition that entangling operations between photons be linearly accessible is generally found to be severely restricting [17–23].

III. NUMERICAL SIMULATION OF LINEAR OPTICAL DEVICES

For an optical circuit made up of K components,

$$A(U_K)A(U_{K-1})\dots A(U_1) = A(U_1U_2\dots U_K). \quad (7)$$

It is preferred to compile the optical hardware components via the matrix multiplication $U_1U_2\dots U_K$, rather than render each $A(U_k)$ independently. The proof of Eq. (7) appears in Appendix A.

Rewriting Eq. (1) as

$$|\psi\rangle = \sum_{\vec{n}} c_{\vec{n}} |\vec{n}\rangle, \quad (8)$$

where

$$|\vec{n}\rangle = |n_1, n_2, \dots, n_M\rangle \quad (9)$$

are the Fock states, we define

$$|\vec{m}(\vec{n})\rangle = |m_1, m_2, \dots, m_N\rangle \quad (10)$$

where m_α is the mode-location of photon number α . Of course the choice of vector $|\vec{m}(\vec{n})\rangle$ for a given $|\vec{n}\rangle$ is not unique, since photons are indistinguishable and labeling them is an arbitrary process. We simply need to choose *some* labeling and pick any valid $|\vec{m}(\vec{n})\rangle$ for each $|\vec{n}\rangle$. Then the elements of $A(U)$ in the basis $|\vec{n}'\rangle\langle\vec{n}|$ are given by

$$A(U)_{\vec{n}',\vec{n}} = \prod_{p=1}^M \frac{\sqrt{n_p!}}{\sqrt{n_p!}} \left[\sum_{\text{perm}(\vec{m}')} U_{m_1m'_1} U_{m_2m'_2} \dots U_{m_Nm'_N} \right], \quad (11)$$

where the summation is over all distinct permutations of integer entries in the vector \vec{m}' . The proof of Eq. (11) appears in Appendix B.

In practice, the input state $|\psi\rangle$ to an optical circuit will often be a simple product state with a definite number of photons in each mode, e.g. $|N, 0, \dots, 0_M\rangle$. Furthermore, a partial measurement on the output state $|\psi'\rangle$ will leave us in some relevant subspace of the full Hilbert space. We can then formally state the following facts.

Fact 1: If the input states $|\psi\rangle$ to our optical circuit are known to be limited to some subspace of the full Hilbert space of the system, we need only build the relevant columns of $A(U)$.

Fact 2: If the output states $|\psi'\rangle$ of our optical circuit are then projected onto some subspace of the full Hilbert space, we need only build the relevant rows of $A(U)$.

With Eq. (7), Eq. (11) and the *Facts*, we can now present our protocol for simulating a linear optical quantum circuit.

Initialization Stage:

- (1) Establish the Fock basis $\{|\vec{n}\rangle\}$ of our input state $|\psi\rangle$. Include only the basis states having nonzero overlap with $|\psi\rangle$, as per *Fact 1*.
- (2) For each element of the basis set $|\vec{n}\rangle$ construct a corresponding $|\vec{m}(\vec{n})\rangle$ as defined in Eq. (10).
- (3) Establish the Fock basis $\{|\vec{n}'\rangle\}$ of our output state $|\psi'\rangle$. Do not include basis states that will be projected out in the measurement, as per *Fact 2*.
- (4) For each element of the basis set $|\vec{n}'\rangle$ construct a corresponding $|\vec{m}'(\vec{n}')\rangle$ as defined in Eq. (10).
- (5) Store all $\vec{n}, \vec{n}', \vec{m}, \vec{m}'$ as integer vectors.

Rendering Stage:

- (1) Compile the total optical circuit composed of K components by performing the matrix multiplication $U = U_1U_2\dots U_K$.
- (2) Render the matrix representation of the quantum operator $A(U)$ using Eq. (11) for all of the relevant input basis states $\{|\vec{n}\rangle\}$ and all of the relevant output basis states $\{|\vec{n}'\rangle\}$.

Initialization needs only to be performed once; we can then quickly build $A(U)$ for any particular optical circuit design, U . This allows fast, repeated simulation

necessary for Monte Carlo applications or numerical optimization. For an open source implementation of this algorithm, see Ref. [24].

IV. RAIL ENCODING QUBITS INTO DETERMINISTIC BLOCKS

It is well established that we can implement any quantum transformation acting on states in the Fock basis using linear optical components if only a single photon is in the system [3–5]:

$$\text{If } N = 1, \quad \mathbf{A} = \mathbf{U}(d_H). \quad (12)$$

That is, we can build a universal quantum computer or fully decodable quantum channel in a single-photon rail encoding. However, by forcing $N = 1$, we sacrifice the scalability of our hardware; Eq. (2) simplifies to

$$d_H = M. \quad (13)$$

To implement j qubits, we need $M = 2^j$ optical modes. Here, we propose grouping single-photon blocks of logical qubits together in order to establish scalability; we want to extend the applicability of single-photon computing to general, large-scale quantum algorithms.

As an example, two qubits can be encoded into an $N = 1, M = 4$ system as shown in Table I. We can then encode

Logical Qubit State	Physical Fock State
$ 00\rangle$	$ 1, 0, 0, 0\rangle$
$ 01\rangle$	$ 0, 1, 0, 0\rangle$
$ 10\rangle$	$ 0, 0, 1, 0\rangle$
$ 11\rangle$	$ 0, 0, 0, 1\rangle$

TABLE I: Two qubits encoded into a single-photon block.

four qubits into the $N = 2, M = 8$ system partitioned into two blocks as described in Table II. In this encoding, we can apply any single-qubit rotation or a controlled-Unitary gate between logical qubits 1 and 2 or between logical qubits 3 and 4 through deterministic manipulation of a single photon [1, 3, 8, 12, 15]. The difficulty here lies in the application of entangling operations between blocks. For example, we may want to apply the $\text{CNOT}_{1,4}$ gate meaning that the control is logical qubit 1 and the target is logical qubit 4. This operation requires the two photons in our system to interact; if a photon is contained in modes 3 or 4, we swap a photon between modes 5 and 6 or between modes 7 and 8.

Generalizing the 2-qubit block encoding in Table I, we can encode q qubits into a block of 1 photon in 2^q modes. Again, operations between pairs of logical qubits contained entirely within in a block are simple to implement using linear optics, but we will need to test our ability to realize communication between blocks. We assume a mapping between logical qubit states and Fock states

Logical Qubit State	Physical Fock State
$ 0000\rangle$	$ 1, 0, 0, 0, 1, 0, 0, 0\rangle$
$ 0001\rangle$	$ 1, 0, 0, 0, 0, 1, 0, 0\rangle$
$ 0010\rangle$	$ 1, 0, 0, 0, 0, 0, 1, 0\rangle$
$ 0011\rangle$	$ 1, 0, 0, 0, 0, 0, 0, 1\rangle$
$ 0100\rangle$	$ 0, 1, 0, 0, 1, 0, 0, 0\rangle$
$ 0101\rangle$	$ 0, 1, 0, 0, 0, 1, 0, 0\rangle$
$ 0110\rangle$	$ 0, 1, 0, 0, 0, 0, 1, 0\rangle$
$ 0111\rangle$	$ 0, 1, 0, 0, 0, 0, 0, 1\rangle$
$ 1000\rangle$	$ 0, 0, 1, 0, 1, 0, 0, 0\rangle$
$ 1001\rangle$	$ 0, 0, 1, 0, 0, 1, 0, 0\rangle$
$ 1010\rangle$	$ 0, 0, 1, 0, 0, 0, 1, 0\rangle$
$ 1011\rangle$	$ 0, 0, 1, 0, 0, 0, 0, 1\rangle$
$ 1100\rangle$	$ 0, 0, 0, 1, 1, 0, 0, 0\rangle$
$ 1101\rangle$	$ 0, 0, 0, 1, 0, 1, 0, 0\rangle$
$ 1110\rangle$	$ 0, 0, 0, 1, 0, 0, 1, 0\rangle$
$ 1111\rangle$	$ 0, 0, 0, 1, 0, 0, 0, 1\rangle$

TABLE II: Four qubits encoded into two single-photon blocks.

Logical Qubit State	Physical Fock State
$ 0 \dots 00\rangle$	$ 1, 0, 0, 0, \dots, 0\rangle$
$ 0 \dots 01\rangle$	$ 0, 1, 0, 0, \dots, 0\rangle$
$ 0 \dots 10\rangle$	$ 0, 0, 1, 0, \dots, 0\rangle$
$ 0 \dots 11\rangle$	$ 0, 0, 0, 1, \dots, 0\rangle$
\vdots	\vdots
$ 1 \dots 11\rangle$	$ 0, 0, 0, 0, \dots, 1\rangle$

TABLE III: q qubits encoded into a single-photon block.

within a single block as in Table III. Without loss of generality, we can group two blocks together, choose the first qubit in the control block as a control qubit, and the last qubit in the target block as a target qubit. Then, we can generalize the $\text{CNOT}_{1,4}$ gate to the $\text{CNOT}_{\text{first},\text{last}}$ gate, which swaps adjacent modes in the target block if a photon is in the second half of the modes in the control block. This operation cannot be implemented through vanilla linear optics:

$$\text{CNOT}_{\text{first},\text{last}} \notin \mathbf{A}. \quad (14)$$

In the special case $q = 1$, our block encoding reduces to the standard dual-rail encoded qubit [1]. In the KLM [6, 7] scheme, the $\text{CNOT}_{\text{first},\text{last}}$ gate can be applied to dual-rail qubits using probabilistic partial measurements with success probability $p = 2/27$.

V. ELEMENTARY PHOTON-ENTANGLING OPERATIONS

In practice, we find it useful to dismantle the $\text{CNOT}_{\text{first},\text{last}}$ gate into a set of elementary entangling

sub-operations. We can first examine the \mathcal{C}_1 sub-operation acting on three modes as defined in Table IV. Here, the first mode is a control mode, while the second

$$\begin{aligned}
|0, 0, 0\rangle &\rightarrow |0, 0, 0\rangle \\
|0, 0, 1\rangle &\rightarrow |0, 0, 1\rangle \\
|0, 1, 0\rangle &\rightarrow |0, 1, 0\rangle \\
|1, 0, 0\rangle &\rightarrow |1, 0, 0\rangle \\
|1, 0, 1\rangle &\rightarrow |1, 1, 0\rangle \\
|1, 1, 0\rangle &\rightarrow |1, 0, 1\rangle
\end{aligned}$$

TABLE IV: The \mathcal{C}_1 operation acting on three modes expressed as a transformation of Fock basis states. The first mode acts as the control while the second and third modes act as targets. We can build the $\text{CNOT}_{\text{first, last}}$ gate by applying this operation 2^{2q-2} times for block size $q \geq 1$.

and third modes are target modes. We apply the \mathcal{C}_1 operator four times to build the $\text{CNOT}_{1,4}$ in $q = 2$, where in each sub-operation the control mode takes values 3 or 4 in Table II and the pair of target modes takes values 5, 6 or 7, 8. The end result is the $\text{CNOT}_{1,4}$ operation: If a photon is in mode 3 or 4 we swap a photon between mode 5 and mode 6 or a photon between mode 7 and mode 8. More generally, a $\text{CNOT}_{\text{first, last}}$ gate for block size q can be constructed by applying the \mathcal{C}_1 operation 2^{2q-2} times by setting the control mode to each of the modes in the second half of the control block, and the two target modes to every sequential pair of modes in the target block. Because there will never be more than a single photon in a block, the basis states in Table IV will be the only possible inputs to the \mathcal{C}_1 transformation. If \mathcal{C}_1 is performed correctly, photon leakage between blocks cannot occur. Other entangling sub-operations we study here include the \mathcal{C}_2 , \mathcal{C}_3 , and \mathcal{C}_4 gates which are presented in Tables V-VII. As the sub-operations get increasingly more complex, a smaller number of such sub-operations is required to implement the inter-block logical operation $\text{CNOT}_{\text{first, last}}$.

The focus of our work here is to test our ability to build these operators as probabilistic measurement-assisted transformations. By this, we mean that we augment our optical computational state $|\psi_c\rangle$ with an ancilla state $|\psi_a\rangle$, apply a linear optical transformation, and then perform a partial projective measurement (refer to Fig. 1). The total action of this non-unitary process can be written formally as a Kraus operator we call $PAULA$, which acts on any input optical quantum state $|\psi_c\rangle$ composed of N_c photons in M_c modes contained in the computational subspace:

$$E = PA(U)L_a \quad (15)$$

$$|\psi'_c\rangle = \frac{E|\psi_c\rangle}{\sqrt{\langle\psi_c|E^\dagger E|\psi_c\rangle}}. \quad (16)$$

$$|0, 0, 0, 0\rangle \rightarrow |0, 0, 0, 0\rangle$$

$$\begin{aligned}
|0, 0, 0, 1\rangle &\rightarrow |0, 0, 0, 1\rangle \\
|0, 0, 1, 0\rangle &\rightarrow |0, 0, 1, 0\rangle \\
|0, 1, 0, 0\rangle &\rightarrow |0, 1, 0, 0\rangle \\
|1, 0, 0, 0\rangle &\rightarrow |1, 0, 0, 0\rangle
\end{aligned}$$

$$\begin{aligned}
|1, 0, 0, 1\rangle &\rightarrow |1, 0, 1, 0\rangle \\
|1, 0, 1, 0\rangle &\rightarrow |1, 0, 0, 1\rangle \\
|0, 1, 0, 1\rangle &\rightarrow |0, 1, 1, 0\rangle \\
|0, 1, 1, 0\rangle &\rightarrow |0, 1, 0, 1\rangle
\end{aligned}$$

TABLE V: The \mathcal{C}_2 operation acting on four modes expressed as a transformation of Fock basis states. The first two modes act as the controls while the last two modes act as targets. We can build the $\text{CNOT}_{\text{first, last}}$ gate by applying this operation 2^{2q-3} times for block size $q \geq 2$.

$$\begin{aligned}
|0, 0, 0, 0, 0\rangle &\rightarrow |0, 0, 0, 0, 0\rangle \\
|0, 0, 0, 0, 1\rangle &\rightarrow |0, 0, 0, 0, 1\rangle \\
|0, 0, 0, 1, 0\rangle &\rightarrow |0, 0, 0, 1, 0\rangle \\
|0, 0, 1, 0, 0\rangle &\rightarrow |0, 0, 1, 0, 0\rangle \\
|0, 1, 0, 0, 0\rangle &\rightarrow |0, 1, 0, 0, 0\rangle \\
|1, 0, 0, 0, 0\rangle &\rightarrow |1, 0, 0, 0, 0\rangle \\
|1, 0, 0, 0, 1\rangle &\rightarrow |1, 0, 0, 1, 0\rangle \\
|1, 0, 0, 1, 0\rangle &\rightarrow |1, 0, 0, 0, 1\rangle \\
|1, 0, 1, 0, 0\rangle &\rightarrow |1, 1, 0, 0, 0\rangle \\
|1, 1, 0, 0, 0\rangle &\rightarrow |1, 0, 1, 0, 0\rangle
\end{aligned}$$

TABLE VI: The \mathcal{C}_3 operation acting on five modes expressed as a transformation of Fock basis states. The first mode acts as the control while the last four modes act as targets. We can build the $\text{CNOT}_{\text{first, last}}$ gate by applying this operation 2^{2q-3} times for block size $q \geq 2$.

In Eq. (15), L_a is the operator defined by

$$L_a|\psi_c\rangle = |\psi_a\rangle \otimes |\psi_c\rangle \quad \forall |\psi_c\rangle, \quad (17)$$

where $|\psi_a\rangle$ is a normalized ancilla state composed of N_a photons in M_a optical modes. The matrix representation of L_a is sparse and satisfies $L_a^\dagger L_a = I$. $A(U)$ is the standard unitary linear optical transformation as defined in Eq. (11), where $N = N_c + N_a$ and $M = M_c + M_a$. P is a partial projective measurement over the ancilla modes. We assume the projection operator P is given by

$$P = |\vec{n}_a\rangle\langle\vec{n}_a| \otimes I, \quad (18)$$

where $|\vec{n}_a\rangle$ is some Fock state containing the same number of photons N_a and modes M_a as the input ancilla state $|\psi_a\rangle$. E therefore preserves photon and mode num-

$$|0, 0, 0, 0, 0, 0\rangle \rightarrow |0, 0, 0, 0, 0, 0\rangle$$

$$|0, 0, 0, 0, 0, 1\rangle \rightarrow |0, 0, 0, 0, 0, 1\rangle$$

$$|0, 0, 0, 0, 1, 0\rangle \rightarrow |0, 0, 0, 0, 1, 0\rangle$$

$$|0, 0, 0, 1, 0, 0\rangle \rightarrow |0, 0, 0, 1, 0, 0\rangle$$

$$|0, 0, 1, 0, 0, 0\rangle \rightarrow |0, 0, 1, 0, 0, 0\rangle$$

$$|0, 1, 0, 0, 0, 0\rangle \rightarrow |0, 1, 0, 0, 0, 0\rangle$$

$$|1, 0, 0, 0, 0, 0\rangle \rightarrow |1, 0, 0, 0, 0, 0\rangle$$

$$|0, 1, 0, 0, 0, 1\rangle \rightarrow |0, 1, 0, 0, 1, 0\rangle$$

$$|0, 1, 0, 0, 1, 0\rangle \rightarrow |0, 1, 0, 0, 0, 1\rangle$$

$$|0, 1, 0, 1, 0, 0\rangle \rightarrow |0, 1, 1, 0, 0, 0\rangle$$

$$|0, 1, 1, 0, 0, 0\rangle \rightarrow |0, 1, 0, 1, 0, 0\rangle$$

$$|1, 0, 0, 0, 0, 1\rangle \rightarrow |1, 0, 0, 0, 1, 0\rangle$$

$$|1, 0, 0, 0, 1, 0\rangle \rightarrow |1, 0, 0, 0, 0, 1\rangle$$

$$|1, 0, 0, 1, 0, 0\rangle \rightarrow |1, 0, 1, 0, 0, 0\rangle$$

$$|1, 0, 1, 0, 0, 0\rangle \rightarrow |1, 0, 0, 1, 0, 0\rangle$$

TABLE VII: The \mathcal{C}_4 operation acting on six modes expressed as a transformation of Fock basis states. The first two modes act as the controls while the last four modes act as targets. We can build the $\text{CNOT}_{\text{first, last}}$ gate by applying this operation 2^{2q-4} times for block size $q \geq 2$.

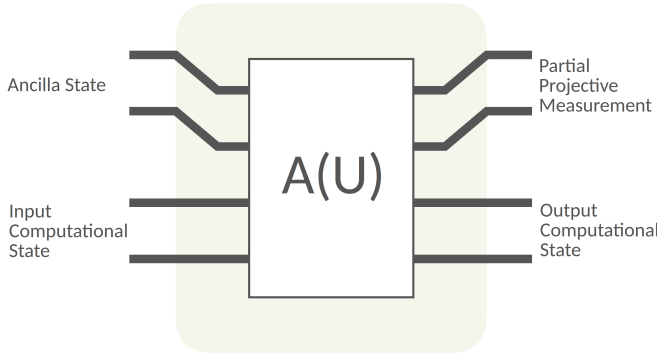


FIG. 1: The measurement-assisted transformation described by E . An input computational state $|\psi_c\rangle$ and ancilla state $|\psi_a\rangle$ are processed through a linear circuit. Then, a partial measurement P is performed and we are left with the output computational state $|\psi'_c\rangle$.

ber. In accordance with *Facts 1* and *2*, we do not construct the entire matrix $A(U)$ – only the columns associated with nonzero components of $L_a |\psi_c\rangle$ and the rows left after the projection P . We define d_c as the dimension of the subspace containing all possible input computational states to our circuit, and d'_c as the full physical Hilbert space associated with the output modes:

$$d'_c = \frac{(N_c + M_c - 1)!}{N_c!(M_c - 1)!}. \quad (19)$$

E can be represented as a d'_c by d_c rectangular matrix.

A measure of gate fidelity (more precisely, the real part

of the fidelity amplitude) between the *PAULA* operator E and a target operation T can be defined by

$$F(E, T) = \frac{\text{Re}[\text{tr}(E^\dagger T)]}{\sqrt{d_c \text{tr}(E^\dagger E)}}. \quad (20)$$

The probability of having successfully applied E for $F(E, T) \rightarrow 1$ is given by

$$S(E) = \frac{\text{tr}(E^\dagger E)}{d_c}. \quad (21)$$

To construct the \mathcal{C}_1 operation defined in Table IV, which acts on input states having 0, 1, or 2 photons, we simultaneously maximize the gate fidelity and success probability for each $N_c = 0, 1, 2$ *separately* over the same quantum optical circuit U and ancilla state $|\psi_a\rangle$. That is, we establish an ideal target T_{N_c} and Kraus *PAULA* operator E_{N_c} for each photon number N_c and attempt to find an optical mode transformation U and ancilla input $|\psi_a\rangle$ such that $F(E_{N_c}, T_{N_c}) \rightarrow 1$ for all N_c with optimal $S(E_{N_c})$. We will demonstrate the details of this in the following section for \mathcal{C}_1 . The same approach is readily extended to $\mathcal{C}_2 \dots \mathcal{C}_4$, and in the following we omit a detailed discussion of the optimization relating to those operators, instead showing only the final results.

VI. NUMERICAL ANALYSIS OF \mathcal{C}_1

We consider first \mathcal{C}_1 acting on the subspace of $N_c = 0$ photons. Here we get the correct transformation for free:

$$|0, 0, 0\rangle \rightarrow |0, 0, 0\rangle. \quad (22)$$

Up to a possible overall phase (see below), this will be the result for any linear optical circuit U and any ancilla state $|\psi_a\rangle$, just because E in this subspace is always a 1 by 1 matrix: $d_c = d'_c = 1$.

If only a single photon is found in the three modes, $N_c = 1$, we have

$$d_c = d'_c = 3, \quad (23)$$

and we strive for a target operator,

$$T_1 = \begin{pmatrix} 1 & 0 & 0 \\ 0 & 1 & 0 \\ 0 & 0 & 1 \end{pmatrix} \quad (24)$$

in the basis

$$\{|\vec{n}_c\rangle\} = \{|\vec{n}'_c\rangle\} = \{|0, 0, 1\rangle, |0, 1, 0\rangle, |1, 0, 0\rangle\}. \quad (25)$$

Finally, in the two-photon subspace, $N_c = 2$, we have

$$d_c = 2 \quad d'_c = 6, \quad (26)$$

and strive for a target operator,

$$T_2 = \begin{pmatrix} 0 & 1 \\ 1 & 0 \\ 0 & 0 \\ 0 & 0 \\ 0 & 0 \\ 0 & 0 \end{pmatrix} \quad (27)$$

in the basis

$$\{|\vec{n}_c\rangle\} = \{|1, 0, 1\rangle, |1, 1, 0\rangle\} \quad (28)$$

$$\begin{aligned} \{|\vec{n}'_c\rangle\} &= \{|1, 0, 1\rangle, |1, 1, 0\rangle, \\ &|2, 0, 0\rangle, |0, 2, 0\rangle, |0, 1, 1\rangle, |0, 0, 2\rangle\}. \end{aligned} \quad (29)$$

We define the *PAULA* operators $E_{N_c}(U, \psi_a)$ separately for the $N_c = 0$, $N_c = 1$ and $N_c = 2$ subspaces, and numerically maximize the function

$$f(U, \psi_a) = \sum_{N_c=0}^2 \left[F(E_{N_c}, T_{N_c}) + \epsilon S(E_{N_c}) \right] \quad (30)$$

where $\epsilon > 0$ is a real-valued numerical weight for the optimization, or equivalently a Lagrange multiplier. We systematically vary parameters ϵ , N_a , M_a , and partial measurement P , and repeat maximization of Eq. (30) to find global solutions.

Any difference in global phases between the operations in Eqs. (22), (24), and (27) will cause an unwanted relative phase shift between Fock basis states in the full transformation \mathcal{C}_1 . For this reason, we use the gate fidelity amplitude defined in Eq. (20), which accounts for a global phase difference between E and T .

VII. RESULTS

A. The entangling operation \mathcal{C}_1

The physical operation \mathcal{C}_1 acting on three modes is of particular importance; it can be applied once to two qubits encoded in the dual rail ($q = 1$) in order to apply an entangling CNOT gate between the two qubits. Numerical optimization of Eq. (30) leads to the same optimal solution as the one given in [25], with two ancilla photons in two modes:

$$\begin{aligned} F(E_{N_c}, T_{N_c})_{\max} &= 1 \\ S(E_{N_c})_{\max} &= 2/27 \\ N_a &= M_a = 2 \\ P &= |11\rangle\langle 11|. \end{aligned} \quad (31)$$

Increasing the number of ancilla resources beyond $N_a = M_a = 2$ does not improve the success probability for numerically accessible ancilla sizes ($N_a, M_a \leq 8$). Thus, for a block size of $q \geq 1$ qubits, we find a maximum

probability of successfully applying a $\text{CNOT}_{\text{first, last}}$ gate composed of \mathcal{C}_1 operations using measurement-assisted transformations to be

$$p = (2/27)^{2^{2q-2}}. \quad (32)$$

B. The entangling operation \mathcal{C}_2

We find the optimal solution:

$$\begin{aligned} F(E_{N_c}, T_{N_c})_{\max} &= 1 \\ S(E_{N_c})_{\max} &= 0.0221391 \\ N_a &= 3, M_a = 4 \\ P &= |1110\rangle\langle 1110|. \end{aligned} \quad (33)$$

For a block size of $q \geq 2$ qubits, we find a maximum probability of successfully applying a $\text{CNOT}_{\text{first, last}}$ gate composed of \mathcal{C}_2 operations using measurement-assisted transformations to be

$$p = (0.0221391)^{2^{2q-3}}. \quad (34)$$

C. The entangling operation \mathcal{C}_3

We find the optimal solution:

$$\begin{aligned} F(E_{N_c}, T_{N_c})_{\max} &= 1 \\ S(E_{N_c})_{\max} &= 0.0221266 \\ N_a &= 3, M_a = 4 \\ P &= |1110\rangle\langle 1110|. \end{aligned} \quad (35)$$

For a block size of $q \geq 2$ qubits, we find a maximum probability of successfully applying a $\text{CNOT}_{\text{first, last}}$ gate composed of \mathcal{C}_3 operations using measurement-assisted transformations to be

$$p = (0.0221266)^{2^{2q-3}}. \quad (36)$$

D. The entangling operation \mathcal{C}_4

We find the optimal solution:

$$\begin{aligned} F(E_{N_c}, T_{N_c})_{\max} &= 1 \\ S(E_{N_c})_{\max} &= 0.00691511 \\ N_a &= M_a = 4 \\ P &= |1111\rangle\langle 1111|. \end{aligned} \quad (37)$$

For a block size of $q \geq 2$ qubits, we find a maximum probability of successfully applying a $\text{CNOT}_{\text{first, last}}$ gate composed of \mathcal{C}_4 operations using measurement-assisted transformations to be

$$p = (0.00691511)^{2^{2q-4}}. \quad (38)$$

VIII. DISCUSSION

We observe a promising increase in success probability of applying the $\text{CNOT}_{\text{first,last}}$ gate as we move to sub-operations acting on a greater number of modes; refer to Fig. 2. Even within the reach of our numerical simula-

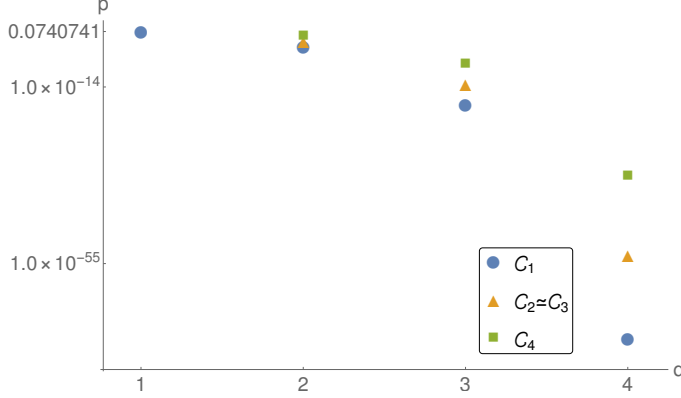


FIG. 2: Maximized success probabilities p for implementing a full $\text{CNOT}_{\text{first,last}}$ gate composed entirely of the sub-operations C_1, C_2, C_3, C_4 , for blocks encoding q qubits.

tions, we find an improvement over standard KLM for applying entangling operations within the context of some quantum algorithms. For example, the simple quantum circuit

$$\text{CNOT}^3 = (I \otimes I \otimes \text{CNOT}) \cdot (I \otimes \text{CNOT} \otimes I) \cdot (\text{CNOT} \otimes I \otimes I) \quad (39)$$

acting on four qubits is presented in Fig. 3. Through the standard KLM protocol acting on qubits encoded in the dual-rail, each CNOT gate can be implemented with success probability $2/27$ using ancilla resources $N_a = M_a = 2$. The total success probability of the CNOT^3 gate using KLM is then $(2/27)^3$ using ancilla resources $N_a = M_a = 6$. Grouping these four qubits into two deterministic blocks of two qubits, $q = 2$, we can apply the same operation with a success probability of 0.00691511 using ancilla resources $N_a = M_a = 4$. This is almost a twenty-fold improvement, while using a smaller ancilla resource.

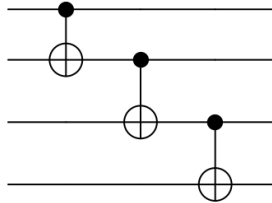


FIG. 3: The quantum circuit CNOT^3 acting on four qubits.

The trend in Fig. 2 suggests an order of magnitude improvement in success probability as we increase the

size (i.e., number of modes operated on) of entangling sub-operations between blocks. Future work can further increase the simulation size to confirm this trend. A high probability $\text{CNOT}_{\text{first,last}}$ gate built from larger sub-operations for block size $q \geq 3$ would have significant implications for linear optical quantum computing.

Acknowledgments

We are thankful for helpful discussions with S. Kaminisky, E. Knutson, and J. Shipman. This research was supported in part using high performance computing (HPC) resources and services provided by Technology Services at Tulane University, New Orleans, LA.

Appendix A: Proof of Eq. (7)

Eq. (7) can be proved by induction. The base case is trivial; for a lone unitary matrix U_1 , Eq. (7) reads

$$A(U_1) = A(U_1). \quad (A1)$$

We can then assume

$$A(U_{K-1})A(U_{K-2}) \dots A(U_1) = A(U_1 U_2 \dots U_{K-1}). \quad (A2)$$

That is, applying the left hand side of (A2) is equivalent to the total transformation

$$\hat{a}_\alpha^\dagger \rightarrow \sum_\beta (U_1 U_2 \dots U_{K-1})_{\alpha,\beta} \hat{a}_\beta^\dagger. \quad (A3)$$

Now we add one final optical component and apply the transformation $A(U_K)$. Our total transformation is now

$$\hat{a}_\alpha^\dagger \rightarrow \sum_\beta (U_1 U_2 \dots U_{K-1})_{\alpha,\beta} \left(\sum_\gamma U_{\beta,\gamma}^K \hat{a}_\gamma^\dagger \right), \quad (A4)$$

where $U_{\beta,\gamma}^K$ are the β, γ elements of U_K . Then,

$$\hat{a}_\alpha^\dagger \rightarrow \sum_{\beta,\gamma} (U_1 U_2 \dots U_{K-1})_{\alpha,\beta} U_{\beta,\gamma}^K \hat{a}_\gamma^\dagger \quad (A5)$$

$$= \sum_\gamma (U_1 U_2 \dots U_K)_{\alpha,\gamma} \hat{a}_\gamma^\dagger, \quad (A6)$$

which is equivalent to $A(U_1 U_2 \dots U_K)$. ■

Appendix B: Proof of Eq. (11)

We can write Eq. (8) in the $|\vec{m}(\vec{n})\rangle$ basis:

$$|\psi\rangle = \sum_{\vec{n}} c_{\vec{n}} |\vec{m}(\vec{n})\rangle. \quad (B1)$$

We note that because of photon indistinguishability, the mapping from $|\vec{n}\rangle$ to $|\vec{m}(\vec{n})\rangle$ is not unique. This mapping

is, however, injective. No matter which of the allowed mappings we choose, no information about the state $|\psi\rangle$ is lost. Thus, we are free to pick any mapping we want for each basis Fock state. Then

$$|\psi\rangle = \sum_{\vec{n}} \frac{\vec{c}_{\vec{n}}}{\prod_{p=1}^M \sqrt{n_p!}} \hat{a}_{m_1}^\dagger \hat{a}_{m_2}^\dagger \dots \hat{a}_{m_N}^\dagger |\vec{0}\rangle. \quad (\text{B2})$$

We define the operators

$$\hat{U}_\alpha = U_{\alpha 1} \hat{a}_1^\dagger + U_{\alpha 2} \hat{a}_2^\dagger \dots U_{\alpha M} \hat{a}_M^\dagger. \quad (\text{B3})$$

Then

$$|\psi'\rangle = A(U) |\psi\rangle = \sum_{\vec{n}} \frac{c_{\vec{n}}}{\prod_{p=1}^M \sqrt{n_p!}} \hat{U}_{m_1} \hat{U}_{m_2} \dots \hat{U}_{m_N} |\vec{0}\rangle. \quad (\text{B4})$$

The product of operators \hat{U}_α in (B4) will return a massive expression of M^N terms. We can use the commutativity of the creation operators

$$[\hat{a}_i^\dagger, \hat{a}_j^\dagger] = 0 \quad \forall i, j \quad (\text{B5})$$

to compress it:

$$|\psi'\rangle = \sum_{\vec{n}} \frac{c_{\vec{n}}}{\prod_{p=1}^M \sqrt{n_p!}} \cdot \sum_{\substack{1 \leq m'_1 \leq \dots \\ \leq m'_N \leq M}} \left[\sum_{\text{perm}(\vec{m}')} U_{m_1 m'_1} \dots U_{m_N m'_N} \right] \hat{a}_{m'_1}^\dagger \dots \hat{a}_{m'_N}^\dagger |\vec{0}\rangle. \quad (\text{B6})$$

Finally, we use

$$\hat{a}_{m'_1}^\dagger \dots \hat{a}_{m'_N}^\dagger |\vec{0}\rangle = \prod_{p=1}^M \sqrt{n'_p(\vec{m}')!} |\vec{n}'(\vec{m}')\rangle \quad (\text{B7})$$

to obtain

$$|\psi'\rangle = \sum_{\vec{n}} c_{\vec{n}} \sum_{1 \leq m'_1 \leq \dots \leq m'_N \leq M} \left[\prod_{p=1}^M \frac{\sqrt{n'_p(\vec{m}')!}}{\sqrt{n_p!}} \right] \left[\sum_{\text{perm}(\vec{m}')} U_{m_1 m'_1} \dots U_{m_N m'_N} \right] |\vec{n}'(\vec{m}')\rangle. \quad (\text{B8})$$

We recognize Eq. (B8) as the result of a matrix-vector product, Eq. (5), if we define $A(U)$ as in Eq. (11). ■

-
- [1] P. Kok, W. J. Munro, K. Nemoto, T. C. Ralph, J. P. Dowling, and G. J. Milburn, *Rev. Mod. Phys.* **79**, 135 (2007).
 - [2] C. K. Hong, Z. Y. Ou, and L. Mandel, *Phys. Rev. Lett.* **59**, 2044 (1987).
 - [3] N. J. Cerf, C. Adami, and P. G. Kwiat, *Phys. Rev. A* **57**, R1477(R) (1998).
 - [4] P. Törmä and S. Stenholm, *Phys. Rev. A* **54**, 4701 (1996).
 - [5] T. B. Pittman, M. J. Fitch, B. C. Jacobs, and J. D. Franson, *Phys. Rev. A* **68**, 032316 (2003).
 - [6] E. Knill, R. Laflamme, G. J. Milburn, *Nature (London)* **409**, 46 (2001).
 - [7] C. R. Myers and R. Laflamme, *arXiv:quant-ph/0512104* (2005).
 - [8] X.-H. Bao, T.-Y. Chen, Q. Zhang, J. Yang, H. Zhang, T. Yang, and J.-W. Pan, *Phys. Rev. Lett.* **98**, 170502 (2007).
 - [9] R. Stárek, M. Mičuda, M. Miková, I. Straka, M. Dušek, M. Ježek and J. Fiurášek, *Scientific Reports* **6**, 33475 (2016).
 - [10] J. T. Barreiro, N. K. Langford, N. A. Peters, and P. G. Kwiat, *Phys. Rev. Lett.* **95**, 260501 (2005).
 - [11] T. M. Graham, H. J. Bernstein, T.-C. Wei, M. Junge, and P. G. Kwiat, *Nat. Commun.* **6**, 7185 (2015).
 - [12] B. P. Lanyon, M. Barbieri, M. P. Almeida, T. Jennewein, T. C. Ralph, K. J. Resch, G. J. Pryde, J. L. O'Brien, A. Gilchrist, and A. G. White, *Nature Physics* **5**, 134 (2009).
 - [13] A. Schreiber, K. N. Cassemiro, V. Potoček, A. Gábris, P. J. Mosley, E. Andersson, I. Jex, and Ch. Silberhorn, *Phys. Rev. Lett.* **104**, 050502 (2010).
 - [14] L. Sansoni, F. Sciarrino, G. Vallone, P. Mataloni, A. Crespi, R. Ramponi, and R. Osellame, *Phys. Rev. Lett.* **108**, 010502 (2012).
 - [15] I. M. Zadeh, A. W. Elshaari, K. D. Jöns, A. Fognini, D. Dalacu, P. J. Poole, M. E. Reimer, and V. Zwiller, *Nano Lett.* **16**, 2289 (2016).
 - [16] M. Reck, A. Zeilinger, H. J. Bernstein, and P. Bertani, *Phys. Rev. Lett.* **73**, 58 (1994).
 - [17] D. B. Uskov, A. M. Smith, and L. Kaplan, *Phys. Rev. A* **81**, 012303 (2010).
 - [18] P. Kok and S. L. Braunstein, *Phys. Rev. A* **62**, 064301 (2000).
 - [19] J. A. Smith, D. B. Uskov, and L. Kaplan, *Phys. Rev. A* **92**, 022324 (2015).
 - [20] P. Lougovski and D. B. Uskov, *Phys. Rev. A* **92**, 022303 (2015).
 - [21] N. Lütkenhaus, J. Calsamiglia, and K.-A. Suominen, *Phys. Rev. A* **59**, 3295 (1999).
 - [22] A. Carollo and G. M. Palma, *J. Mod. Opt.* **49**, 1147 (2002).
 - [23] M. Pavičić, *Phys. Rev. Lett.* **107**, 080403 (2011) (retracted).
 - [24] <https://github.com/jsmith74/linear-optics>
 - [25] D. B. Uskov, L. Kaplan, A. M. Smith, S. D. Huver, and

J. P. Dowling, Phys. Rev. A **79**, 042326 (2009).